DALTON
FULL PAPER

Synthesis and characterization of a novel one-dimensional iron phosphate: $[C_4H_{12}N_2]_{1.5}[Fe_2(OH)(H_2PO_4)(HPO_4)_2(PO_4)]\cdot 0.5H_2O$

Vítìzslav Zima † and Kwang-Hwa Lii ‡

Institute of Chemistry, Academia Sinica, Taipei, Taiwan, R.O.C.

Received 2nd June 1998, Accepted 30th October 1998

An organically templated Fe^{III} phosphate, $[C_4H_{12}N_2]_{1.5}[Fe_2(OH)(H_2PO_4)(HPO_4)_2(PO_4)]\cdot 0.5H_2O$, has been synthesized under hydrothermal conditions and characterized by single-crystal X-ray diffraction, Mössbauer spectroscopy and thermogravimetric analysis. The compound crystallizes in the triclinic space group $P\bar{1}$ (no. 2) with $a = 6.3347(2)$, $b = 13.0075(4)$, $c = 13.7810(5)$ Å, $\alpha = 62.834(1)$, $\beta = 81.404(1)$, $\gamma = 82.688(1)°$, $U = 996.67(8)$ Å^3 and $Z = 2$. The compound is unusual in that it is not only one of the few examples of 1-D organically templated iron phosphate, but also has a new type of chain structure which is built up from tetranuclear iron–oxygen clusters. The tetramer involves an edge-sharing dimer which further links at the shared corners to two more octahedra. These clusters are connected into the 1-D chain by PO_4 tetrahedra and have terminal HPO_4 and H_2PO_4 groups, with the piperazinium cations between the chains.

Introduction

Organically templated transition metal phosphates are of intense current interest because of their novel structures and potential applications as solid catalysts. The first such metallophosphates were prepared with vanadium and molybdenum.[1,2] Recently, a number of iron phosphates and fluorophosphates have been reported.[3–5] They exhibit a wide structural diversity; many adopt 3-D frameworks and 2-D sheets, whilst few have 1-D chain structures. It makes sense in terms of bond-valence theory that 1-D structures are the least common. For P^{5+} every oxide ligand receives a bond-valence contribution of 1.25 v.u. from the central cation, leaving 0.75 v.u. to be supplied by the rest of the structures. Thus most of the phosphates are highly polymerized, being dominated by frameworks and sheets, irrespective of any other variables that may also influence the stoichiometry and structure.[6] To our knowledge $[(1R,2R)\text{-}C_6H_{10}(NH_2)_2][Fe(OH)(HPO_4)_2]\cdot H_2O$, $[trans\text{-}1,2\text{-}C_6H_{10}(NH_2)_2][Fe(OH)(HPO_4)_2]\cdot H_2O$, and $[C_3H_{12}N_2][FeF(HPO_4)_2]\cdot xH_2O$ are the only 1-D organically templated iron phosphates (FePOs).[7,3] Their structures consist of $[FeX(HPO_4)_2]^{2-}{}_n$ (X = OH, F) chains of the tanocoite type, with the diprotonated amines inserted in between. In this paper we report the synthesis and structural characterization of a new 1-D FePO templated with piperazinium cations, $[C_4H_{12}N_2]_{1.5}[Fe_2(OH)(H_2PO_4)(HPO_4)_2(PO_4)]\cdot 0.5H_2O$, which contains a novel infinite chain constructed from phosphate groups and tetranuclear iron–oxygen clusters, and show through Mössbauer measurements that it is an iron(III) compound. The tetranuclear cluster has been observed in the iron phosphate mineral leucophosphite[8] and in the synthetic iron phosphate $[H_3N(CH_2)_3NH_3]_2[Fe_4(OH)_3(HPO_4)_2(PO_4)_3]\cdot xH_2O$.[5]

Experimental

Synthesis

The synthesis was carried out in Teflon-lined acid digestion bombs with an internal volume of 23 cm^3 under autogeneous pressure by heating the starting mixtures at 110 °C for 4 d followed by slow cooling to room temperature at 5 °C h^{-1}. Small colorless prismatic crystals of $[C_4H_{12}N_2]_{1.5}[Fe_2(OH)(H_2PO_4)(HPO_4)_2(PO_4)]\cdot 0.5H_2O$ and large colorless crystals of piperazinium hydrogenphosphate monohydrate, $(C_4H_{12}N_2)\cdot HPO_4\cdot H_2O$,[9] were obtained as the major products from a reaction mixture of $FeCl_3\cdot 6H_2O$ (1 mmol), H_3PO_4 (6 mmol), piperazine (6 mmol), and 10 ml of H_2O. Subsequently, hydrothermal treatment of $FeCl_3\cdot 6H_2O$ (1 mmol), H_3PO_4 (6 mmol), piperazine (6 mmol), and 10 ml of a mixture of water and ethylene glycol (volume ratio 1 : 1) under the same reaction conditions gave a pure product of the title compound, as indicated by a comparison of the X-ray powder pattern to that simulated from the atomic coordinates derived from a single-crystal study. The IR spectrum was also measured. However, we are unable to clearly identify the three types of phosphates from the spectrum because the ν(P–O) bands overlap, ν(OH) bands are weak and broad, and all the phosphates and the water molecule are involved in an extensive hydrogen bonding network. Elemental analysis confirmed the stoichiometry (Found: C, 11.32; H, 3.73; N, 6.22; P, 18.81; Fe, 16.89. Theoretical: C, 11.02; H, 3.70; N, 6.43; P, 18.95; Fe, 17.08%). The yield was 46% based on iron.

TGA and Mössbauer spectroscopy

Thermogravimetric analysis was performed on a Perkin-Elmer TGA 7 thermal analyzer. The sample was heated to 900 °C at 10 °C min^{-1} in flowing oxygen. The final decomposition products were identified by powder X-ray diffraction. The ^{57}Fe Mössbauer measurements were made on a constant-acceleration instrument at 300 K. Isomer shift is reported with respect to an iron foil standard.

Single-crystal X-ray diffraction

A colorless prismatic crystal of dimensions of 0.1 × 0.05 × 0.05 mm was selected for indexing and intensity data collection on a Siemens Smart-CCD diffractometer equipped with a normal focus, 3 kW sealed tube X-ray source. Intensity data were collected in 2082 frames with increasing ω (width of 0.3° per frame). Number of measured reflections and observed unique reflections ($F_o > 4\sigma(F_o)$): 10301 and 2546. $R_{int} = 0.0786$. Empirical absorption corrections were applied using the SADABS program[10] for Siemens area detector ($T_{min,max} = 0.772$,

† On leave from Joint Laboratory of Solid State Chemistry, University of Pardubice, Czech Republic.
‡ *Present address*: Department of Chemistry, National Central University, Chungli, Taiwan 320, R.O.C.

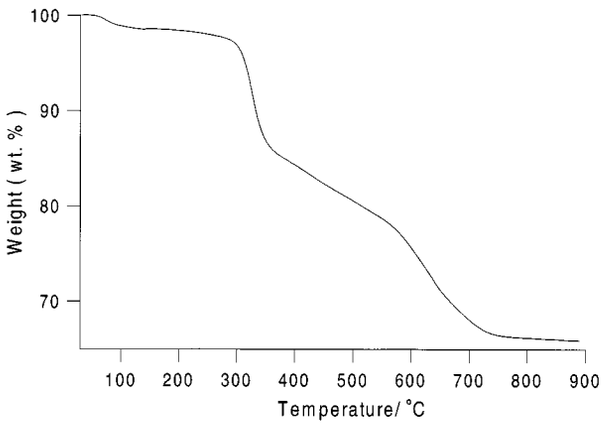

Fig. 1 Thermogravimetric analysis of $[C_4H_{12}N_2]_{1.5}[Fe_2(OH)(H_2PO_4)(HPO_4)_2(PO_4)]\cdot 0.5H_2O$ in flowing oxygen at 10 °C min^{-1}.

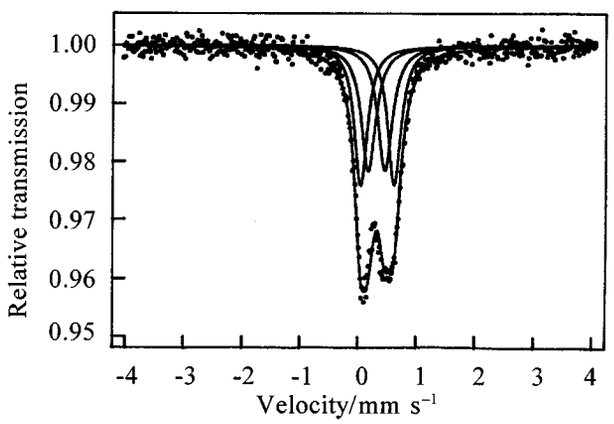

Fig. 2 Mössbauer spectrum of $[C_4H_{12}N_2]_{1.5}[Fe_2(OH)(H_2PO_4)(HPO_4)_2(PO_4)]\cdot 0.5H_2O$ at 300 K.

Table 1 Crystallographic data for $[C_4H_{12}N_2]_{1.5}[Fe_2(OH)(H_2PO_4)(HPO_4)_2(PO_4)]\cdot 0.5H_2O$

Formula	$C_6Fe_2H_{24}N_3O_{17.5}P_4$
M	653.86
Crystal system	Triclinic
Space group	$P\bar{1}$
a/Å	6.3347(2)
b/Å	13.0075(4)
c/Å	13.7810(5)
α/°	62.834(1)
β/°	81.404(1)
γ/°	82.688(1)
V/Å^3	996.67(8)
Z	2
D_c/g cm^{-3}	2.179
F(000)	666
μ(Mo-Kα)/cm^{-1}	18.7
T/°C	23
λ/Å	0.71073
Maximum 2θ/°	57.6
Reflections collected	10301
Unique reflections	4708
Observed unique reflections [$I > 2\sigma(I)$]	2546
Number of parameters	317
$R1$ [a]	0.0512
$wR2$ [b]	0.1226
Goodness of fit	1.114
$(\Delta\rho)_{max,min}$/e Å^{-3}	0.90, −0.55

[a] $R1 = \Sigma||F_o| - |F_c||/\Sigma|F_o|$. [b] $wR2 = \{\Sigma[w(F_o^2 - F_c^2)^2]/\Sigma[w(F_o^2)^2]\}^{\frac{1}{2}}$, where $w = 1/[\sigma^2(F_o^2) + (0.0592P)^2 + 2.36P]$ with $P = (\max F_o^2 + 2F_c^2)/3$.

0.928). On the basis of statistics of intensity distribution and successful solution and refinement of the structure, the space group of the title compound was determined to be $P\bar{1}$ (no. 2). The structure was solved by direct methods. The metal and phosphorus atoms were first located, and the oxygen, nitrogen, and carbon atoms were found in difference Fourier maps. The hydrogen atoms were not located. The piperazinium cation, which is centered at (0,1/2,0), is disordered over two positions with equal occupancy. The water oxygen Ow initially showed a very large thermal parameter. If the occupancy of Ow is refined, the site occupancy factor obtained is 0.52(1), indicative of a half occupancy of the water of crystallization. The final cycles of least-squares refinement including atomic coordinates and anisotropic thermal parameters for all atoms converged at $R1 = 0.0512$ and $wR2 = 0.1226$. Secondary extinction corrections were applied. Structure solution and refinement were performed by using SHELXTL PC, Version 5.[11]

CCDC reference number 186/1227.

Results and discussion

TGA and Mössbauer measurements

Several mass loss regions are seen in TGA of the title compound (Fig. 1). The first mass loss (≈77 °C) corresponds to loss of lattice water molecule. It is interesting that this mass loss occurs below the boiling point of water. We can attribute this facile loss to the low degree of hydrogen bonding holding the water in the crystal lattice. The observed mass loss between 30 and 150 °C is 1.40% and corresponds to 0.5 mol of H_2O per formula unit (calc. 1.38%). The next mass loss (≈325 °C), which is not well resolved from the final steps, is probably due to dehydration of OH^- and hydrogen phosphate groups and deprotonation of piperazinium dications (loss calculated, 11.0%; observed between 150 and 350 °C, 11.9.%). The final steps correspond to the release of organic components, giving $Fe(PO_3)_3$ and $Fe_4(P_2O_7)_3$ as the final decomposition products as indicated by powder X-ray diffraction.[12] The observed total weight loss of 33.8% is close to that calculated for the loss of 27 H_2O and 9 piperazine molecules (32.16%), as indicated by the following equation.

$$6\,[C_4H_{12}N_2]_{1.5}[Fe_2(OH)(H_2PO_4)(HPO_4)_2(PO_4)]\cdot 0.5H_2O \longrightarrow 4\,Fe(PO_3)_3 + 2\,Fe_4(P_2O_7)_3 + 27\,H_2O + 9\,C_4H_{10}N_2$$

The room temperature Mössbauer spectrum (Fig. 2) was least-squares fitted by two doublets with a constraint on the area ratio of 1:1. The obtained parameters are δ (isomer shift) = 0.417 mm s^{-1}, ΔE_Q (quadrupole splitting) = 0.279 mm s^{-1} and Γ (full width at half height) = 0.30 mm s^{-1} for Fe(1) and $\delta = 0.433$ mm s^{-1}, $\Delta E_Q = 0.583$ mm s^{-1} and $\Gamma = 0.27$ mm s^{-1} for Fe(2). The isomer shifts of both contributions are characteristic of high spin Fe^{III}. The higher value of quadrupole splitting of Fe(2) is because of the greater octahedral distortion due to edge-sharing. Therefore, the composition of the title compound is further defined by TG analysis and Mössbauer spectroscopy.

Crystal structure

The crystallographic data are listed in Table 1. The bond lengths, and bond-valence sums are given in Table 2. All atoms are in general positions. There are three independent piperazinium cations. The occupancy factors of N(3a), N(3b), C(6) and C(7) are 0.5 because the piperazinium cation which is centered at (0,1/2,0) is disordered over two positions. The site occupancy factor of the water of crystallization is 0.5. Valence sum calculations[13] show the Fe atoms to possess an oxidation state of 3+. Both Fe atoms are octahedrally coordinated. Atoms O(1), O(3), O(4), O(5), O(8), O(13), O(16) and O(17) have valence sums of 1.42, 1.15, 1.13, 1.33, 1.08, 1.33, 1.08 and 1.00, respectively, and all other oxygen atoms have values close to 2. The valence sums of O(1), O(5) and O(13) are satisfied by forming hydrogen bonds (see below). Atoms O(3), O(4), O(8), O(16) and O(17) are hydroxo oxygens. Therefore the compound contains $H_2P(1)O_4$, $HP(2)O_4$, $P(3)O_4$ and $HP(4)O_4$ groups. Atom O(17) is the hydroxo oxygen bridging three iron atoms.

Table 2 Selected bond lengths (Å) and bond-valence sums (Σs) for $[C_4H_{12}N_2]_{1.5}[Fe_2(OH)(H_2PO_4)(HPO_4)_2(PO_4)]\cdot 0.5H_2O$

Fe(1)–O(2)	1.978(5)	Fe(1)–O(7^{i})	2.007(5)
Fe(1)–O(9^{ii})	1.942(5)	Fe(1)–O(10)	1.997(5)
Fe(1)–O(14)	2.012(5)	Fe(1)–O(17)	2.179(5)
Σs(Fe(1)–O) = 3.02			
Fe(2)–O(6^{i})	1.918(5)	Fe(2)–O(11^{iii})	1.999(5)
Fe(2)–O(12)	2.006(5)	Fe(2)–O(15^{iii})	1.898(5)
Fe(2)–O(17)	2.144(5)	Fe(2)–O(17^{iii})	2.172(5)
Σs(Fe(2)–O) = 3.05			
P(1)–O(1)	1.493(5)	P(1)–O(2)	1.520(5)
P(1)–O(3)	1.569(5)	P(1)–O(4)	1.573(5)
Σs(P(1)–O) = 5.00			
P(2)–O(5)	1.511(5)	P(2)–O(6)	1.514(5)
P(2)–O(7)	1.528(5)	P(2)–O(8)	1.581(6)
Σs(P(2)–O) = 5.00			
P(3)–O(9)	1.509(5)	P(3)–O(10)	1.525(5)
P(3)–O(11)	1.550(5)	P(3)–O(12)	1.552(5)
Σs(P(3)–O) = 5.00			
P(4)–O(13)	1.512(5)	P(4)–O(14)	1.524(5)
P(4)–O(15)	1.524(5)	P(4)–O(16)	1.584(5)
Σs(P(4)–O) = 4.97			
N(1)–C(1)	1.51(1)	N(1)–C(2^{iv})	1.502(9)
C(1)–C(2)	1.52(1)	N(2)–C(3^{ii})	1.51(1)
N(2)–C(4)	1.50(1)	C(3)–C(4^{v})	1.53(1)
N(3a)–C(5^{vi})	1.56(2)	N(3a)–C(6^{vii})	1.50(3)
N(3b)–C(5)	1.47(2)	N(3b)–C(7)	1.46(3)
C(5)–C(6)	1.51(3)	C(5)–C(7^{viii})	1.59(2)

Symmetry codes: (i) x, $y+1$, z; (ii) $x+1$, y, z; (iii) $-x$, $-y+2$, $-z+1$; (iv) $-x+2$, $-y+1$, $-z+1$; (v) $-x+1$, $-y+2$, $-z$; (vi) x, y, $z-1$; (vii) $-x$, $-y+1$, $-z+1$; (viii) $-x$, $-y+1$, $-z+2$.

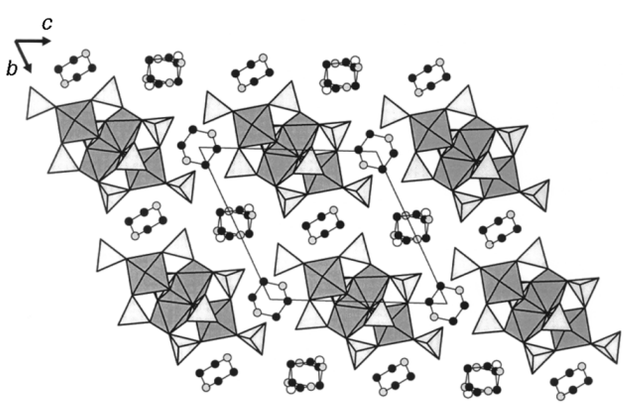

Fig. 3 Structure of $[C_4H_{12}N_2]_{1.5}[Fe_2(OH)(H_2PO_4)(HPO_4)_2(PO_4)]\cdot 0.5H_2O$ viewed along the [100] direction. The piperazinium cation, which is centered at (0,1/2,0), is disordered over two positions. Solid circles, C atoms; stippled circles, N atoms; open circles, water oxygens.

The structure consists of 1-D infinite chains of iron phosphate parallel to the [100] direction, which are H-bonded with the amine groups of piperazinium cations (Fig. 3). The water molecule is also H-bonded as inferred from Ow···N(3a) (2.70 Å) and Ow···O(16) (2.87 Å). The basic building unit of the chain is a tetranuclear iron–oxygen cluster, which is shown in Fig. 4. The cluster consists of two central FeO_6 octahedra that share a common edge, with the two hydroxo oxygens involved in the shared edge serving as corners for two additional FeO_6 octahedra. The tetramer possesses $\bar{1}$ symmetry located at the midpoint of the shared edge. Based on the Fe–O distances, the $Fe(2)O_6$ octahedron appears more distorted than $Fe(1)O_6$ because of edge-sharing. These tetranuclear clusters

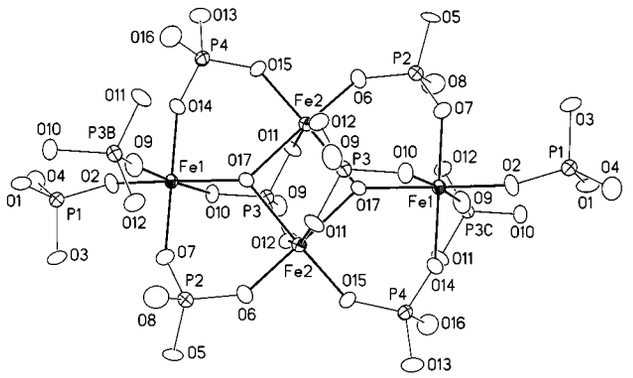

Fig. 4 Tetranuclear iron cluster in $[C_4H_{12}N_2]_{1.5}[Fe_2(OH)(H_2PO_4)(HPO_4)_2(PO_4)]\cdot 0.5H_2O$. Filled lines and single lines are for Fe–O and P–O bonds, respectively. Thermal ellipsoids are shown at 60% probability.

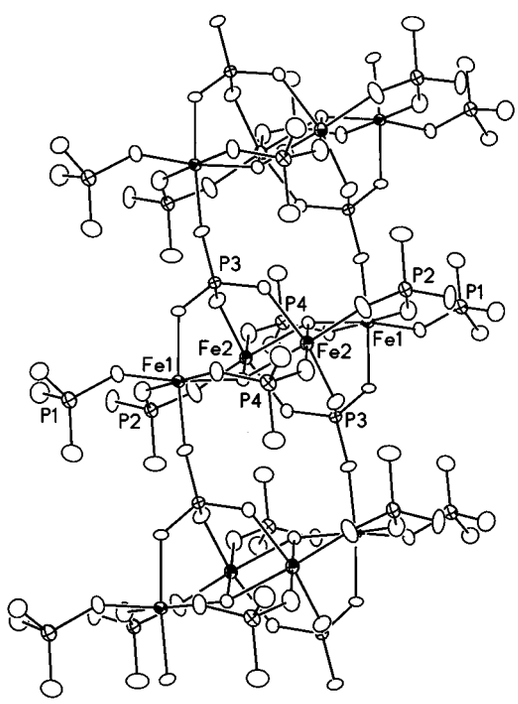

Fig. 5 Section of the infinite chain in $[C_4H_{12}N_2]_{1.5}[Fe_2(OH)(H_2PO_4)(HPO_4)_2(PO_4)]\cdot 0.5H_2O$ showing the connectivity between tetranuclear clusters.

are connected in a 1-D chain by PO_4 tetrahedra and have terminal H_2PO_4 and HPO_4 groups (Fig. 5). The phosphate tetrahedra that complete the building unit are of three types. $H_2P(1)O_4$ has one oxygen, O(2), bridging to Fe(1) and extends away from the cluster as a pendant group. Of the three remaining P(1)–O bonds, one receives hydrogen bonds from neighboring piperazinium cations [O(1)···N(1) 2.657 Å, O(1)···N(2) 2.734 Å], whilst the other two with longer bonds [P(1)–O(3) 1.569 Å, P(1)–O(4) 1.573 Å] constitute P–OH groups. $HP(2)O_4$ and $HP(4)O_4$ groups share two corners of two octahedra within a tetramer with one corner as a terminal hydroxo group and the remaining corner serving as H-bond acceptor from piperazinium cations and H_2PO_4 groups [O(5)···O(3) 2.502 Å, O(5)···N(3a) 2.688 Å, O(13)···O(4) 2.519 Å, O(13)···N(3b) 2.780 Å]. The third type of phosphate, $P(3)O_4$, shares three corners with three octahedra within a tetramer, and one corner with one octahedron in a neighboring tetramer. A topologically identical iron–oxygen cluster exists in the 3-D networks of the mineral leucophosphite, $K_2[Fe_4(OH)_2(H_2O)_2(PO_4)_4]\cdot 2H_2O$, and the synthetic compound $[H_3N(CH_2)_3NH_3]_2[Fe_4(OH)_3(HPO_4)_2(PO_4)_3]\cdot xH_2O$. In leucophosphite the tetramer is coordinated by four PO_4 tetrahedra, each sharing either two or three corners with the FeO_6 octahedra of a

tetramer. One vertex of each corner-sharing octahedron is occupied by a terminal water molecule. In $[H_3N(CH_2)_3NH_3]_2$-$[Fe_4(OH)_3(HPO_4)_2(PO_4)_3]\cdot xH_2O$, the terminal aqua ligand in leucophosphite is replaced by a doubly bridging OH group which connects adjacent tetramers *via* –Fe–O(H)–Fe– bonds forming orthogonal, but non-intersecting infinite chains.

Conclusion

The hydrothermal synthesis described in this work produces another example of iron phosphate with an encapsulated piperazinium cation. The molecule piperazine is a versatile agent which directs the formation of 3-D framework, 2-D layered and 1-D chain structures.[7] There was only one known chain iron phosphate structure containing octahedrally co-ordinated iron centers. The 1-D FePOs $[(1R,2R)$-$C_6H_{10}(NH_2)_2]$-$[Fe(OH)(HPO_4)_2]\cdot H_2O$, $[trans$-$1,2$-$C_6H_{10}(NH_2)_2][Fe(OH)$-$(HPO_4)_2]\cdot H_2O$ and $[C_3H_{12}N_2][FeF(HPO_4)_2]\cdot xH_2O$ all contain $[FeX(HPO_4)_2]^{2-}{}_n$ (X = OH, F) chains of the tanocoite type. The title compound presents a new type of chain architecture which is formed from tetranuclear iron–oxygen clusters.

Acknowledgements

We thank the Institute of Chemistry, Academia Sinica, National Science Council (NSC-87-2113-M-001-019), and Chinese Petroleum Corp. for support, Ms. F.-L. Liao and Professor S.-L. Wang at the National Tsing Hua University for X-ray intensity data collection, and Professor T.-Y. Dong at the National Sun Yat-Sen University for Mössbauer spectroscopy measurements.

References

1 R. C. Haushalter and L. A. Mundi, *Chem. Mater.*, 1992, **4**, 31.
2 M. I. Khan, L. M. Meyer, R. C. Haushalter, A. L. Schweitzer, J. Zubieta and J. L. Dye, *Chem. Mater.*, 1996, **8**, 43.
3 M. Cavellec, D. Riou, J. M. Greneche and G. Ferey, *Inorg. Chem.*, 1997, **36**, 2187.
4 J. R. D. DeBord, W. M. Reiff, C. J. Warren, R. C. Haushalter and J. Zubieta, *Chem. Mater.*, 1997, **9**, 1994.
5 K.-H. Lii and Y.-F. Huang, *Chem. Commun.*, 1997, 839.
6 F. Hawthorne, *Z. Kristallogr.*, 1990, **192**, 1.
7 K.-H. Lii, Y.-F. Huang, V. Zima, C.-Y. Huang, H.-M. Lin, Y.-C. Jiang, F.-L. Liao and S.-L. Wang, *Chem. Mater.*, 1998, **10**, 2599.
8 P. B. Moore, *Am. Mineral.*, 1972, **57**, 397.
9 D. Riou, T. Loiseau and G. Ferey, *Acta Crystallogr.*, *Sect. C*, 1993, **49**, 1237.
10 G. M. Sheldrick, SADABS, Empirical Absorption Corrections Program, University of Göttingen, 1997.
11 G. M. Sheldrick, SHELXTL PC, Version 5, Siemens Analytical X-Ray Instruments Inc., Madison, WI, 1994.
12 $Fe(PO_3)_3$, file number 38–109; $Fe_4(P_2O_7)_3$, 36–318; Joint Committee on Powder Diffraction Standards, International Center of Diffraction Data, Swarthmore, PA.
13 I. D. Brown and D. Altermatt, *Acta Crystallogr.*, *Sect. B*, 1985, **41**, 244.

Paper 8/04143A